HHS Public Access

Author manuscript

Cell Rep. Author manuscript; available in PMC 2018 May 13.

Published in final edited form as:

Cell Rep. 2018 January 16; 22(3): 611–623. doi:10.1016/j.celrep.2017.12.079.

INO80 Chromatin Remodeling Coordinates Metabolic Homeostasis with Cell Division

Graeme J. Gowans[1], **Alicia N. Schep**[2], **Ka Man Wong**[1], **Devin A. King**[1], **William J. Greenleaf**[2], and **Ashby J. Morrison**[1,3,*]

[1]Department of Biology, Stanford University, Stanford, CA 94305, USA

[2]Department of Genetics, Stanford University, Stanford, CA 94305, USA

SUMMARY

Adaptive survival requires the coordination of nutrient availability with expenditure of cellular resources. For example, in nutrient-limited environments, 50% of all *S. cerevisiae* genes synchronize and exhibit periodic bursts of expression in coordination with respiration and cell division in the yeast metabolic cycle (YMC). Despite the importance of metabolic and proliferative synchrony, the majority of YMC regulators are currently unknown. Here, we demonstrate that the INO80 chromatin-remodeling complex is required to coordinate respiration and cell division with periodic gene expression. Specifically, INO80 mutants have severe defects in oxygen consumption and promiscuous cell division that is no longer coupled with metabolic status. In mutant cells, chromatin accessibility of periodic genes, including TORC1-responsive genes, is relatively static, concomitant with severely attenuated gene expression. Collectively, these results reveal that the INO80 complex mediates metabolic signaling to chromatin to restrict proliferation to metabolically optimal states.

Graphical abstract

In Brief: Gowans et al. reveal that the INO80 complex is needed to coordinate cell division with nutrient availability in *S. cerevisiae*. In metabolically synchronized INO80 mutants, oscillations of metabolic gene expression and chromatin accessibility are severely attenuated compared with wild-type cells.

*Correspondence: ashbym@stanford.edu.
[3]Lead Contact

Data and Software Availability

GSE101290

AUTHOR CONTRIBUTIONS

Conceptualization and Methodology, A.J.M. and G.J.G.; Investigation, G.J.G.; Formal Analysis and Visualization, G.J.G., A.N.S., and K.M.W.; Resources, D.A.K.; Writing – Original Draft, A.J.M. and G.J.G.; Writing – Review & Editing, A.J.M., G.J.G., K.M.W., and D.A.K.; Supervision, A.J.M. and W.J.G.; Funding Acquisition, A.J.M.

SUPPLEMENTAL INFORMATION

Supplemental Information includes five figures and five tables and can be found with this article online at https://doi.org/10.1016/j.celrep.2017.12.079.

DECLARATION OF INTERESTS

The authors declare no competing interests.

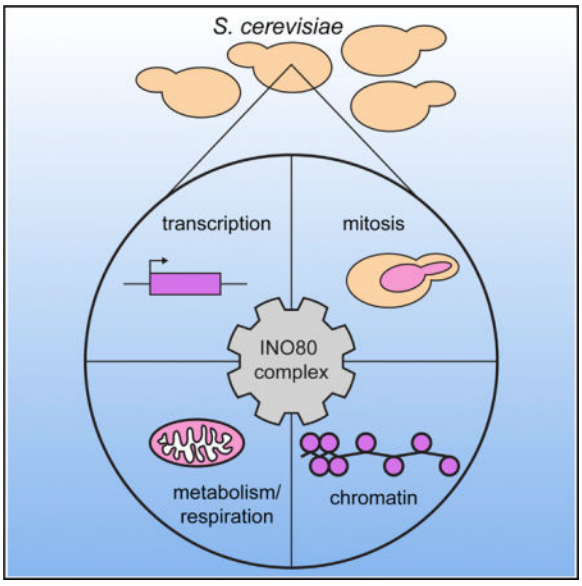

INTRODUCTION

The coordination of cellular function with the environment is essential for adaptation and survival. Cells and organisms have a remarkable ability to sense diverse (i.e., nutrient-rich or -limiting) environments and reprogram their energy metabolism and proliferative capacity accordingly. Limiting nutrient environments are ubiquitous throughout nature and range from competitive microorganism growth environments to niches surrounding developing tissues in multicellular organisms. Failure to adapt can lead to cell death, developmental defects, and disease. Indeed, energy metabolism alterations are a major contributing factor to many pathologies, including cancer, cardiovascular disease, and diabetes, which together account for approximately half of all deaths in the United States (Centers for Disease Control and Prevention, 2015).

Adaptive cellular responses are often achieved by rapid inducible changes in gene expression (López-Maury et al., 2008). For example, metabolic adaptation in the budding yeast *Saccharomyces cerevisiae* is achieved, in part, by coordinated regulation of gene expression, cell division, and metabolic status in low-nutrient environments that mimic natural environments in the wild. Under such glucose-deprived conditions, yeasts quickly synchronize their metabolic processes and undergo coordinated and periodic bursts of respiration during a phenomenon known as the yeast metabolic cycle (YMC) (Klevecz et al., 2004;Tu et al., 2005).

In the YMC, over half of all transcripts undergo periodic expression (Figure 1A; Table S1). For example, genes involved in protein synthesis are induced during the high oxygen consumption (HOC) or oxidative (OX) phase. Following the OX phase, during the low oxygen consumption (LOC) or reductive building (RB) phase, genes involved in DNA replication and mitochondrial biogenesis are upregulated. Subsequently, genes involved in glycolysis and the environmental stress response are upregulated during periods of LOC in the reductive charging (RC) phase. This temporal organization facilitates “just in time”

coordination of cellular function, wherein genes are transcribed just prior to the utilization of their encoded proteins within a particular metabolic or cell cycle pathway (Kuang et al., 2014;McAdams and Shapiro, 2003;Wang et al., 2015;Zaslaver et al., 2004). Furthermore, periodically expressed genes in multiple species are among the most energetically expensive to transcribe and translate (Wagner, 2005;Wang et al., 2015). As such, coordinated periodic transcription, rather than constitutive expression, maximizes the efficiency of limited cellular resources.

Importantly, periodic gene expression is an evolutionarily conserved process. These highly robust gene expression cycles are observed in both lab and wild prototrophic yeast strains and in single cells from asynchronous populations (Burnetti et al., 2016;Laxman et al., 2010;Silverman et al., 2010). Similarly, mammals undergo circadian rhythms, with oscillations in gene transcription and metabolic pathways coordinated with the day/night cycle (Panda, 2016). Analysis of the mouse transcriptome across multiple tissues revealed that 43% of protein-coding genes exhibit circadian rhythm-driven expression oscillations (Zhang et al., 2014).

Tight regulation of periodic gene expression not only promotes metabolic efficiency, as previously mentioned, but also optimizes cell growth and division. This is evident by the temporal constraint of cell division in both the circadian cycle and YMC (Burnetti et al., 2016;Klevecz et al., 2004;Matsuo et al., 2003;Nagoshi et al., 2004;Tu et al., 2005). In specific prototrophic strains, cell division is gated within the RB phase of the YMC, purportedly to shield replicating DNA from genotoxic reactive oxygen species (Chen et al., 2007). In addition, cell cycle start is coupled to the initiation of the OX phase in several yeast strains, likely to ensure that cell division occurs following the accumulation of sufficient energy reserves (Burnetti et al., 2016). Cell division frequency can be dynamically altered by nutrient availability and is absent without metabolic oscillations (Papagiannakis et al., 2017;Robertson et al., 2008). These studies highlight the critical importance of coordinating cell growth and division with metabolic environments.

Although the importance of synchronous metabolic and cell division oscillations is becoming increasingly clear, the identification of regulatory mechanisms for these processes is currently lacking. However, an emerging concept is that chromatin modification is an ideal mechanism to orchestrate gene expression in coordination with the metabolic environment (Gut and Verdin, 2013). This is primarily because many chromatin modifiers are abundant, regulate a large number of genes, and require intermediary metabolites as enzymatic cofactors. Thus, they can “communicate” metabolic status to the global chromatin environment. Moreover, epigenetic alterations can be rapidly and reversibly induced and are capable of dynamically directing gene expression in coordination with changing nutrient environments.

We have recently identified the evolutionarily conserved INO80 complex as a regulator of metabolic function (Yao et al., 2016). The INO80 chromatin-remodeling complex restructures and repositions nucleosomes *in vitro* (Gerhold and Gasser, 2014;Morrison and Shen, 2009). *In vivo*, INO80 is enriched at the +1 nucleosome that plays critical roles in defining chromatin accessibility at promoters (Yao et al., 2016;Yen et al., 2012). The *S.*

cerevisiae INO80 chromatin remodeler is composed of 15 subunits (Shen et al., 2000) that constitute four structurally distinct subunit modules along the Ino80 ATPase (Tosi et al., 2013;Watanabe et al., 2015). We found that the Arp5-Ies6 module, which is needed for chromatin remodeling catalytic activity (Shen et al., 2003;Tosi et al., 2013;Watanabe et al., 2015;Yao et al., 2015), regulates the expression of genes in energy metabolism pathways. Specifically, *arp5Δ* mutants display an upregulation of genes involved in the oxidative phosphorylation pathway (Yao et al., 2016). Accordingly, mitochondrial potential and oxygen consumption are altered in *arp5Δ*, *ies6Δ*, and *ino80Δ* mutants.

To further investigate the relationship between INO80 and metabolic homeostasis, we examined the effect of INO80 deletion on metabolic and cell division oscillations in the YMC. In this report, we show that deletion of INO80 subunits severely disrupts metabolic cycling. Furthermore, we demonstrate that the INO80 complex is needed for robust TORC1-mediated gene expression, which is critical for YMC maintenance. Finally, we show that disruption of the INO80 complex decouples cell division from metabolic oscillations. Collectively, our results establish the INO80 complex as a key regulator of metabolism that integrates nutrient signaling with gene expression and cell growth.

RESULTS

The INO80 Complex Is Essential for Respiration Oscillations

To determine the role of INO80 in the YMC, we analyzed the effect of genetic disruption of each of the unique, non-essential subunits of the INO80 complex on YMC respiratory oscillations. We found that deletion of the Ino80 ATPase subunit had the most severe effect on YMC organization because the culture rapidly lost the ability to periodically respire but maintained a constitutively high rate of oxygen consumption (Figure 1B). These results are consistent with previous observations that INO80 chromatin remodeling and nucleosome assembly factors are needed to repress genes in the oxidative phosphorylation pathway (Galdieri et al., 2016;Yao et al., 2016).

Deletion of *ARP8* resulted in a metabolic cycle that prematurely entered the OX phase at the midpoint of RC. Although not as severe as the *ino80Δ* mutant, deletion of either *ARP5* or *IES6* resulted in rapid oscillations in oxygen consumption (Figure 1B), with each cycle lasting approximately half the length of a wild-type cycle. The *arp5Δ* and *ies6Δ* mutants exhibited similar phenotypes in the YMC, consistent with their physical association as a subcomplex both within and outside of the INO80 complex (Tosi et al., 2013;Watanabe et al., 2015;Yao et al., 2015,2016). The difference in YMC length between *arp5Δ* and wild-type strains was largely contributed by a drastically reduced RC (low oxygen consumption) phase. A similar profile was observed for the *ino80Δ* mutant before the cycles ceased (Figure 1B).

Deletion of *IES5* or *NHP10* also disrupted the periodicity of the YMC (Figure S1A). Ies5 is part of the Nhp10 module (Tosi et al., 2013), and purification of the INO80 complex from an *ies5Δ* strain showed a dramatic reduction in Ies1, Ies3, and Nhp10 (Figure S1B), corroborating recent results (Sardiu et al., 2017). Interestingly, deletion of *NHP10* and *IES5* do not result in fitness defects in rich media (Morrison et al., 2007) (A.J.M., unpublished

data), whereas deletion of the catalytic subunits of the INO80 complex, such as *ARP8*, *ARP5*, and *IES6*, reduces fitness (Yao et al., 2016). Nevertheless, *nhp10Δ* and *ies5Δ* mutants both displayed defects in respiration cycles in the YMC. Thus, defects observed in the YMC do not always translate to fitness defects in unsynchronized cells.

Deletion of other subunits of the INO80 complex, including *IES1*, *IES3*, and *IES4*, had only minimal effects on the YMC. A summary of the phenotypes within each structural module is illustrated in Figure 1C. Purification of Ino80-FLAG throughout the YMC from wild-type cells demonstrated that the complex composition is not dramatically altered (i.e., no obvious loss or gain of subunits is observed) during the respiration oscillations (data not shown); thus, reconfiguration of the complex does not appear to regulate normal YMC kinetics. Notably, the YMC defects observed in mutants of the INO80 complex are not common to all remodelers because deletion of *SWR1*, a subunit of the SWR1 chromatin-remodeling complex and another chromatin remodeler in the INO80 subfamily (Mizuguchi et al., 2004), had no effect on the cycle (Figure S1C).

Disruption of the INO80 Complex Alters Global Transcription across the YMC

In asynchronous cultures, the INO80 complex regulates the expression of an abundance of genes enriched in metabolic processes (Yao et al., 2016). To assess differences in transcript levels across the YMC, we performed an RNA sequencing (RNA-seq) analysis of both wild-type and *arp5Δ* cultures at six different time points during the cycle. We selected the *arp5Δ* mutant because it has a severely disrupted profile while still maintaining sufficient cycles for sampling. To examine the relationship between samples, principal-component analysis (PCA) (Ringnér, 2008) was performed. Principal components 1 and 2 revealed that wild-type samples (triangles) are roughly arranged in a circle, mirroring the cyclical nature of the system (Figure 2A). A similar pattern is observed for the *arp5Δ* data (circles), although the samples are noticeably clustered closer together, indicating that the differences between these samples are smaller than the differences observed between the wild-type samples.

To determine whether specific metabolic pathways were misregulated in the *arp5Δ* mutant, we next compared the expression of previously characterized periodic genes (Kuang et al., 2014) within each phase of the YMC (Figure 2B). These genes were identified using a periodicity algorithm on RNA-seq samples compiled at high resolution (16 time points) across the YMC (Kuang et al., 2014). We determined functional annotation enrichments for these periodic genes in wild-type cells (Table S1), which were used as a reference to identify the YMC pathways disrupted in *arp5Δ* mutants.

In the *arp5Δ* strain, although transcripts peaked during the expected phases, expression was markedly attenuated compared with the wild-type. Significant differentially expressed (SDE) gene analysis between the mutant and wild-type during each phase of the YMC supported the observation of “muted” cycles in the *arp5Δ* mutant (Figure 2C; Table S1). For example, pathways with peak expression in the wild-type OX phase, such as ribosome biogenesis, are also expressed in *arp5Δ* mutant at the same time point. However, these transcripts are identified as significantly downregulated compared with wild-type cells because peak expression is dampened in mutant cells (Figure 2C). Conversely, many of these OX phase pathways are comparatively upregulated in the *arp5Δ* mutant during the RB

phase because they are not repressed to the same degree as in wild-type cells. These data demonstrate that, in the *arp5Δ* mutant, periodic genes are generally expressed in the corresponding phase. However, the amplitude of periodic expression is dramatically decreased, resulting in YMC phasing that is less defined.

Cell Division Is Disconnected from the YMC in the arp5D Mutant

Analysis was then performed to identify periodic genes in the *arp5Δ* mutant that do not exhibit expression in the expected YMC phase. Unsupervised clustering (*k*-means) analysis was performed on previously defined periodic genes (Kuang et al., 2014) after normalizing (z-score) by transcript, time point, and strain, adjusting the muted expression defects observed in *arp5Δ* cells. For both wild-type and *arp5Δ* cells, the vast majority of periodic genes (>3,800 genes) clustered into one of three distinct patterns that reflect RC, OX, and RB peak mean expression (Figure 3A; Table S3). This supports the observation that, although gene expression is dramatically muted in *arp5Δ* mutants, periodic expression of many genes is still detectable. However, we identified 722 genes in *arp5Δ* mutants with peak expression and *k*-means clustering in a different phase than expected, representing genes with severe defects in periodic transcriptional regulation (Table S3). Functional annotation analysis demonstrates that these genes are significantly enriched in cell cycle and mitotic pathways (Figure 3B). As previously discussed, cell division and DNA replication are coupled with the RB phase of the YMC in this prototrophic strain (CEN.PK) (Burnetti et al., 2016;Chen et al., 2007;Klevecz et al., 2004;Tu et al., 2005). Additionally, genes involved in mitosis and chromosomal segregation were significantly upregulated in the RC phase of *arp5Δ* cells (Figure 2C). Thus, cell cycle gene expression is dramatically altered in the *arp5Δ* mutant YMC.

To further investigate the disruption of cell cycle kinetics in *arp5Δ* cells, we monitored DNA content and cell budding across the YMC. As reported previously (Tu et al., 2005), the wild-type RB phase was tightly coupled to DNA replication (Figure 3C) and cell division (Figure 3D). However, in the *arp5Δ* mutant, DNA replication was uncoupled from the YMC because we observed a population of cells with 2N DNA content and budding cells at all phases (Figures 3C and 3D). The cell density of the *arp5Δ* culture re actor with constant perfusion of media. Thus, these defects in the *arp5Δ* mutant are not due to cell cycle arrest or cell death. Conversely, these results suggest that disruption of the INO80 complex decouples cell division from the metabolic state of the cell.

Loss of INO80 Function Alters Global Chromatin Accessibility in the YMC

To assess the influence of the INO80 chromatin remodeling in the YMC, we utilized the assay for transposase-accessible chromatin using sequencing (ATAC-seq) (Buenrostro et al., 2015). ATAC-seq uses a hyperactive Tn5 transposase that preferentially inserts specific adaptors in regions of accessible chromatin. Samples were taken at the same time points as for RNA-seq (Figure 2A). Similar to the RNA-seq results, PCA illustrates the cyclical relationship among samples (Figure 4A) within PC2 and PC3, whereas PC1 largely partitioned wild-type and *arp5Δ* samples separately (Figure S2). The distribution of samples in the PCA plot is indicative of periodic fluctuations in chromatin accessibility across the YMC. However, the *arp5Δ* samples were clustered in the center of the plot, suggesting that

the differences between these samples were much less pronounced than in the wild-type (Figure 4A).

To explore potential mechanisms of INO80-mediated transcription regulation, we then investigated ATAC accessibility across all periodic gene promoters, defined as −400 bp downstream and 100 bp upstream of the transcriptional start site (TSS). ATAC scores largely correlated with gene expression (correlation coefficient [*r*] = 0.86 for OX, 0.72 for RC, and 0.99 for RB), with increased accessibility corresponding to the phase of periodic expression (Figure 4B). However, the accessibility of periodic gene promoters was more static in *arp5Δ* cells compared with the wild-type. When accessibility was viewed along individual chromosomes in 500-bp bins, oscillating accessibility was observed in wild-type cells, with relatively decreased accessibility during the RC-to-OX transition and increased accessibility during the RB phase (Figure 4C; Figure S3). However, accessibility along chromosomes in *arp5Δ* cells was much less dynamic during the YMC. Moreover, large domains of relatively accessible (red boxes) or inaccessible (blue boxes) chromatin were observed in *arp5Δ* cells, with corresponding alterations in RNA abundance (Figure 4C; Figure S3). These data reveal that disruption of INO80 chromatin remodeling results in global chromatin accessibility defects that reduce the plasticity of the chromatin template during metabolic oscillations.

Metabolic Gene Promoters Are Dependent on INO80-Facilitated Chromatin Accessibility

To identify individual transcription factors that are influenced by INO80 chromatin remodeling, chromatin accessibility was assessed for promoters of specific transcription factor (TF) motifs. The presence of each annotated transcription factor motif (n = 177) was assessed for all promoters, defined as −400 bp downstream and 100 bp upstream relative to the TSS. The results revealed that, similar to the data in Figure 4A, the wild-type data were much more dynamic than the mutant data (Figure 5A). In particular, several motifs exhibited comparably large fluctuations in accessibility (Figure 5B), suggesting a relatively large dependence on chromatin manipulation for regulation of those genes. Indeed, periodic expression of these highlighted TF-regulated genes is largely coordinated with accessibility in wild-type cells (Figure 5C). However, in the *arp5Δ* mutant, these motifs lacked dynamic accessibility and exhibited significant differential accessibility between wild-type and *arp5Δ* cells (Benjamini-Hochberg-adjusted $p < 0.01$) (Figure 5B). In addition, corresponding gene expression was deregulated (Figure 5C).

Notably, many of these highlighted transcription factor motifs are components of the energy-responsive TORC1 pathway (Figure 5D). For example, under nutrient-rich growth conditions, Msn2/4 are inhibited by TORC1 via phosphorylation, which results in their exclusion from the nucleus (Beck and Hall, 1999). Under nutrient-depleted growth conditions, these transcription factors translocate to the nucleus and express genes in the general stress response (Gasch et al., 2000;Martínez-Pastor et al., 1996;Schmitt and McEntee, 1996). Dot6, Tod6, and Stb3 are phosphorylated by Sch9 in a TORC1-dependent manner to promote expression of ribosomal protein (RP) and ribosome biogenesis (Ribi) gene expression (Huber et al., 2009;2011; Figure 5D). TORC1 also directly phosphorylates the transcriptional activator Sfp1 to facilitate its binding to RP gene promoters and subsequent expression (Lempiäinen et al., 2009;Marion et al., 2004).

Interestingly, Reb1 and Abf1, which are critical factors in controlling nucleosome positioning at promoters (Hartley and Madhani, 2009), are found in the promoters of ribosome biogenesis genes and genes involved in protein and mRNA transport (Figure 5D). Consistent with our observations, a recent study identified Reb1 and Abf1 at ribosome biogenesis promoters using chromatin immunoprecipitation (ChIP) *in vivo* (Bosio et al., 2017). In *arp5Δ* mutant cells, Reb1 and Abf1 motifs were the most significantly statically inaccessible among all motifs and across all phases of the YMC (Benjamini-Hochberg-adjusted $p < 0.001$). Comparatively, in wild-type cells, the Reb1 and Abf1 motifs exhibited coordinated oscillations of accessibility and gene expression in the YMC (Figures 5B and 5C).

We then examined accessibility at high resolution across the motifs of these transcription factors (Figure 5E; Figure S4A). We observed that there were striking phase-dependent differences between wild-type and *arp5Δ* mutant cells. Specifically, when comparing these two strains, the Dot6, Sfp1, Reb1, and Abf1 motifs show the greatest difference in accessibility during the OX phase (Figure 5E). In wild-type cells, this peak of accessibility correlates with the peak of expression of genes containing these motifs in their promoters (Figures 5B and 5C) and likely stems from a shared translation (Figure 5D). Conversely, regions containing Msn2/4 motifs have reduced accessibility during the OX phase, with comparably smaller differences between the wild-type and the *arp5Δ* mutant (Figure 5B). However, at higher resolution, strain-dependent differences are observed within Msn2/4 motifs during the RB and RC phase (Figure 5E). During these phases of the YMC, Msn2/4-dependent gene expression is induced in the wild-type (Figure 5C) and enriched in energy metabolism pathways (Figure 5D). Interestingly, these results suggest that Msn2/4 are not restricted to stress-related gene expression in the YMC. Furthermore, these analyses demonstrate that INO80 activity is necessary to create dynamically accessible chromatin at the motifs of transcription factors important for YMC regulation.

As previously stated, INO80 is a chromatin remodeler that is enriched at the +1 nucleosome (Yao et al., 2016;Yen et al., 2012). Thus, we also assessed promoter-proximal nucleosome positioning across the YMC in both wild-type and *arp5Δ* cells. However, our ability to confidently call nucleosomes was confounded in the *arp5Δ* mutants because of an overall decrease in predicted nucleosome-spanning fragments compared with wild-type samples. The precise origin of this technical limitation is not known. However, it may be a consequence of increased +1 nucleosome “fuzziness”; i.e., deviation in mean nucleosome positioning of individual +1 nucleosomes in a cell population, which was previously observed in *ino80Δ and arp5Δ* mutants (Yao et al., 2016). For +1 nucleosomes that could be confidently called, no statistically significant deviations were detected proximal to transcription factor motifs when comparing wild-type with *arp5Δ* mutants (Figure 5F and data not shown).

However, we did observe a significant change in the −1 nucleosome position for genes containing either the Abf1 or Reb1 transcription factor motifs. We observed differences in the size and significance of the median shift in nucleosome position depending on the motif identification method used. Using the JASPAR database (Mathelier et al., 2016), we observed median shifts of 6 and 4.5 bp in 1 nucleosome position proximal to Abf1 (p =

0.026) and Reb1 (p = 0.158) motifs, respectively (Figure 5F). Using a previously published ChIP analysis in the absence of chromatin crosslinking, occupied regions of genomes from affinity-purified naturally isolated chromatin (ORGANIC) (Kasinathan et al., 2014), we observed median shifts in −1 nucleosome position of 3.5 and 4 bp proximal to Abf1 (p = 0.012) and Reb1 (p = 0.004) motifs, respectively (Figure S4B). No other statistically significant deviations were observed for nucleosomes proximal to other transcription factor motifs (data not shown). These data support a previously unrecognized role for the INO80 complex in −1 nucleosome positioning at specific metabolic promoters.

For most transcription factors, these defects in accessibility, gene regulation, and nucleosome positioning do not appear to be due to general gene expression defects of the transcription factors themselves (Figures S4C and S4D). Although many of these transcription factors display periodic expression, which has been reported previously for Msn4 (Rao and Pellegrini, 2011), the pattern of expression does not always directly correlate with the expression of other genes that have the motif. However, notable exceptions are Tod6 and Sfp1, which have patterns of transcription factor expression that closely mirror the expression of genes with corresponding motifs in their promoters (Figure 5C; Figure S4C). Thus, a portion of the defects in metabolic gene expression and chromatin architecture observed in *arp5Δ* cells may originate with alterations of transcription factor expression itself. However, INO80 chromatin remodeling also plays a major role in regulating the chromatin architecture at the recognition motifs of several metabolic transcription factors. The combined effect of INO80 loss of function is a dramatically unresponsive and static chromatin architecture that does not exhibit periodic regulation characteristics of the YMC.

The INO80 Complex Is a Key Regulator of TORC1-Responsive Gene Expression

Of all transcription factors assessed, Msn2 and Msn4 had the largest ATAC-seq variability across the YMC of wild-type cells, which is altered in the *arp5Δ* mutant (Figure 5B). Because Msn2 and Msn4 are regulated by the TORC1 pathway, we sought to further determine the role of TORC1 in the YMC. We first examined Msn2-mediated transcription in greater detail by restricting the analysis to ChIP-validated Msn2-induced genes following acute glucose deprivation (n = 88) (Elfving et al., 2014). Again, we found that Msn2-dependent genes were markedly reduced in the OX phase of the wild-type YMC (Figure 6A), when accessibility of Msn2 motif-containing genes is lowest (Figure 5B). In the *arp5Δ* mutant, we observed lower expression of these Msn2-induced genes in the RC phase of the cycle (Figure 6A), with generally static accessibility patterns across the entire YMC at corresponding motifs (Figure 5B).

We then examined the requirement for INO80 on all TORC1-regulated gene expression by analyzing the expression of rapamycin-sensitive genes in the YMC. We identified both significantly upregulated (n = 1177) and downregulated (n = 1249) genes from asynchronous cultures treated with rapamycin (Table S4). Analysis of these transcript levels showed that rapamycin-induced genes (TORC1-repressed) have reduced expression during the OX phase (Figure 6A, bottom). The expression pattern of these TORC1-repressed genes closely mirrors the pattern of Msn2-regulatd genes. Conversely, rapamycin-repressed genes (TORC1-induced) have peak expression during the OX phase. In the *arp5Δ* mutant, this

divergent pattern between rapamycin-induced and -repressed expression was much less distinguished, demonstrating that TORC1-regulated gene expression is periodic in the YMC and dependent on INO80-mediated chromatin remodeling.

Overall, gene expression in untreated asynchronous cultures had the strongest correlation with the OX phase of the YMC; however, rapamycin treatment greatly weakened this association (Figure 6B). We then monitored TORC1 signaling by examining the phosphorylation of ribosomal protein S6 (Rps6) (González et al., 2015), a downstream substrate in the TORC1 pathway (Yerlikaya et al., 2016). Rps6 phosphorylation was nearly undetectable in the RC phase of the YMC and peaked during the OX phase of wild-type cells (Figure 6C). These data reinforce the idea of the OX phase being the main TOR-regulated growth phase of the YMC, with the other phases similar to quiescent or stationary phases in asynchronous cultures.

Because of the importance of TORC1 signaling in the YMC, treatment with rapamycin resulted in disruption of the YMC at the point of maximal TOR activity (Figure 6D), confirming previous findings that addition of rapamycin disrupted respiration cycles in the YMC (Murray et al., 2007). Rapamycin treatment prevented the increase in phospho-Rps6 and acetylation of a number of H3 lysine residues, which are known to fluctuate across the YMC (Cai et al., 2011; Figure 6D; data not shown). (Note that rapamycin was prepared in ethanol, which itself can be metabolized, accounting for the transient decrease in dissolved oxygen [dO_2]; addition of ethanol alone had no effect on subsequent cycles; Figure S5A). Addition of acetate has been shown to induce premature entry into OX phase (Cai et al., 2011) and, as we observed, an increase in TOR activity and histone acetylation (Figure S5B). Last, genetic deletion of *SCH9* or *RIM15*, downstream components of the TORC1 pathway (Urban et al., 2007;Wanke et al., 2008), also either prevented or disrupted metabolic cycles (Figure S5C).

As mentioned, TORC1-responsive gene expression is muted in *arp5Δ* cells (Figure 6A). Interestingly, we observed that the induction of TORC1 signaling appeared normal in the *arp5Δ* strain, with a peak in the OX phase, despite the differences in YMC period (Figure 6E). Thus, although upstream TORC1 signaling appears intact in the *arp5Δ* mutant, downstream TORC1-regulated gene expression is disrupted. These results demonstrate that the INO80 complex is a critical effector of TORC1-regulated gene expression that coordinates the quiescence (RC) to growth (OX) transition and maintains metabolic homeostasis.

DISCUSSION

The INO80 Chromatin Remodeler Is a Key Regulator of Metabolic Function

Our data show that the INO80 chromatin-remodeling complex plays a major role in maintaining metabolic homeostasis in yeast. The cumulative defect in *arp5Δ* mutant cells is a system-level disorganization of the metabolic cycle, characterized by severely diminished ability to organize robust YMC phasing and coordinate cell division with metabolic timing.

The resulting effect of INO80 disruption is likely to contribute to metabolic inefficiency, whereby transcripts are produced out of synchrony with the function of the encoded protein. For example, in *arp5Δ* mutants, ribosomal gene expression is both produced (i.e., derepressed) out of phase and not fully activated during the optimal OX phase. Gene expression related to ribosome biogenesis involves nearly 10% of the genome, with many exhibiting more than 40-fold amplitude changes in the YMC. It has been proposed that approximately 60% of total *S. cerevisiae* transcription is devoted to rRNA production and that 50% of RNA polymerase II (Pol II) transcription is involved in ribosomal protein expression (Warner, 1999). Thus, the process of translation creates a tremendous energy expenditure for the cell that must be tightly regulated to ensure efficiency. In the YMC, gene expression programs related to translation peak during the OX phase, coincident with the production of ATP (Machné and Murray, 2012) and acetyl-coenzyme A (CoA) (Cai et al., 2011), which can feed these energy-demanding processes. Because mutants of the INO80 complex do not optimize this energy-demanding process, all cellular processes that require coordination of function with energy availability are likely jeopardized.

Previous research demonstrates that INO80 maintains proper DNA ploidy during cell division (Chambers et al., 2012). In this study, we report unrestricted cell division in *arp5Δ* mutants. The coordination of energy metabolism and cell division is vital to survival in competitive nutrient environments. Moreover, excessive proliferation that is disconnected from nutrient availability is characteristic of diseases such as cancer. For example, the mTOR signaling pathway is often constitutively active in cancer, promoting growth signaling and proliferation irrespective of metabolic environments (Laplante and Sabatini, 2009). In this study, we find that the INO80 complex is a critical component for enacting TOR-responsive transcriptional programs. Interestingly, subunits of the evolutionarily conserved INO80 complex are commonly amplified in many cancers, including 51% of lung squamous cell carcinoma (Cancer Genome Atlas Research Network, 2012), 50% of pancreatic (Witkiewicz et al., 2015), and 45% of bladder cancers (Cancer Genome Atlas Research Network, 2014). The results from this study reveal the INO80 complex as a previously unrecognized regulator of proliferative capacity that restricts cell division to metabolically optimal states. Additional studies may further define the role of INO80 subunits in human metabolism and disease.

The INO80 Complex Regulates the Chromatin Architecture of Metabolic Genes

We observe that chromatin accessibility is dynamically altered in the YMC. Specifically, metabolic promoters exhibit large fluctuations in accessibility that correspond to gene expression. For example, we observed that chromatin accessibility surrounding TORC1-responsive promoters fluctuated across the YMC and was largely static in the *arp5Δ* mutant. Thus, the organization of the YMC is particularly dependent on TORC1-regulated gene expression, which, in turn, is influenced by INO80 chromatin remodeling.

Notably, we also found that Msn2/4-regulated gene expression and ATAC accessibility are dramatically altered in *arp5Δ* mutants. As previously mentioned, Msn2/4 transcription factors are well known to regulate stress responses in a TORC1-dependent manner (Gasch et al., 2000;Martínez-Pastor et al., 1996;Schmitt and McEntee, 1996). For example, in response

to glucose deprivation, Msn2 induces energy metabolism genes, such as those involved in trehalose and glycogen metabolism and oxidation reduction (Elfving et al., 2014). Furthermore, Msn2/4 have recently been found to regulate carbohydrate metabolism and acetyl-CoA abundance in the YMC (Kuang et al., 2017). In this study, we found that Msn2/4-regulated genes are periodically expressed in the YMC and enriched in energy metabolism pathways. Loss of INO80 chromatin remodeling severely diminishes Msn2/4-regulated gene expression, concomitant with attenuated chromatin accessibility at Msn2/4 motifs. It should be noted that INO80 may directly influence TORC1-mediated signaling by altering chromatin at TORC1-responsive loci and/or indirectly by regulating the cellular energetic state.

We also observed dramatically reduced accessibility at Abf1 and Reb1 motif-containing promoters in the *arp5Δ* mutant. These promoters are found at ribosome biogenesis genes, and, in wild-type cells, are among those with the largest fluctuations in accessibility across the YMC. Abf1 and Reb1 play major roles in establishing nucleosomal array positioning at promoters (Hartley and Madhani, 2009). Abf1 motifs are enriched upstream of the TSS (Ganapathi et al., 2011), and Reb1 localizes to the −1 nucleosome (Koerber et al., 2009). We find that INO80 chromatin remodeling is needed to position the −1 nucleosome at promoters that contain Reb1 and Abf1 motifs. Interestingly, most of the −1 nucleosomes bound by Reb1 are found at divergently transcribed genes (Koerber et al., 2009), and disruption of Reb1 function causes a reduction in the expression of these genes (Wang and Donze, 2016). Additionally, loss of Abf1 caused decreased nucleosome occupancy upstream of the TSS (Ganapathi et al., 2011). Our data demonstrate that −1 nucleosome positioning by Abf1 and Reb1-mediated is dependent on INO80 chromatin remodeling, the disruption of which is detrimental for metabolic homeostasis.

It should be noted that some of the YMC defects observed in *arp5Δ* cells may be an indirect result of INO80 dysfunction. For example, *ARP5* deletion may directly result in a shortened RC phase, which consequently results in a relative elongation of the subsequent OX phase. Acute disruption of INO80 function will be needed to resolve direct and indirect YMC effects.

The YMC Is a Powerful Tool for Studying Metabolic Signaling to Chromatin

Our results also demonstrate that chromatin modification is an excellent means to regulate gene expression in coordination with changing metabolic environments. Previous research also supports this model by demonstrating that histone acetylation is tightly coupled to carbon availability (Cai et al., 2011), which is converted to acetyl-CoA, an intermediary metabolite and cofactor for histone acetyltransferases.

It has been proposed that cellular ATP oscillations might influence the activity of ATP-dependent chromatin remodelers during the YMC (Amariei et al., 2014;Machné and Murray, 2012). Considering that there are several thousand chromatin-remodeling enzymes in the cell (Ghaemmaghami et al., 2003) and an order of magnitude more predicted nucleosome substrates, the energy demand of chromatin remodeling may consume a significant amount of cellular resources. OX phase genes exhibit the highest amplitude in gene expression throughout the YMC, which is coincident with the peak of ATP (Machné and Murray, 2012;

A.J.M., unpublished data). It may be that this increase in ATP production provides a metabolically permissive environment to allow extensive chromatin remodeling. Alternatively, when intracellular ATP levels are low, it may limit the amount of chromatin remodeling that can occur across the genome. Indeed, previous research has linked dynamic nucleosome positioning and transcription to respiration oscillations in the YMC (Amariei et al., 2014;Machné and Murray, 2012;Nocetti and Whitehouse, 2016). Future research connecting chromatin modulation with YMC gene expression is likely to further uncover chromatin connections to metabolism.

EXPERIMENTAL PROCEDURES

Yeast Strains and Metabolic Treatment

Saccharomyces cerevisiae strains were constructed in the CEN. PK background using standard genetic techniques (Table S5). Metabolic cycling conditions were performed as described previously (Tu et al., 2005), except that starter cultures were grown in minimal media without sulfuric acid. For RNA-seq analysis of the rapamycin-sensitive transcriptome, the BY4741 strain was used.

Western Blotting

Protein was extracted using an NaOH/tricarboxylic acid (TCA) extraction method. The following antibodies were used in this study: Hxk1 (Novus Biologicals, NB120-20547), Arp5 (Abcam, ab12099), H3 (Active Motif, 39163), acetylated histone H3 lysine 9 (H3K9ac), (Millipore, 06-942), pRps6 (Cell Signaling Technology, 2211), FLAG (Sigma, F1804), and hemagglutinin (HA) (Sigma, 11867423001).

RNA-Seq Analysis

RNA was prepared from samples (1.5 optical density [OD]) using the MasterPure yeast RNA purification kit (Epicenter, MPY03100). The sequencing libraries were prepared from 0.8 μg of RNA/sample using the Illumina TruSeq stranded mRNA kit (Illumina, 15031047). A minimum of 10 million reads per time point were aligned, in duplicate, using Bowtie 2 and analyzed using the DESeq2 package (Love et al., 2014). Replicates were combined for final analysis. Fragments per kilobase of transcript per million mapped reads is abbreviated as FPKM. PCA plots were generated on log-transformed data using the DESeq2 package (Love et al., 2014).

For the transcriptional comparative analysis in Figure 2C, time points with the highest correlation between wild-type and mutant log2-transformed expression within each phase were chosen, which includes the following: wild-type sample 2 versus mutant sample 1 (RC), $r = 0.95$; wild-type sample 3 versus mutant sample 3 (OX), $r = 0.91$; and wild-type sample 6 versus mutant sample 5 (RB), $r = 0.96$. SDE genes (adjusted $p < 0.05$) were identified at each of these time points using the DESeq2 package (Love et al., 2014). Functional annotation analysis was performed on SDE genes using Database for Annotation, Visualization, and Integrated Discovery (DAVID) with default parameters (Huang et al., 2009a;2009b).

Genes expressed in the wild-type YMC were previously determined as “periodic” or “non-periodic” using a periodicity algorithm on RNA-seq compiled at high resolution (16 time points) across the YMC (Kuang et al., 2014; Table S1).

ATAC-Seq Analysis

The ATAC-seq assay and data processing were performed as described previously (Schep et al., 2015). The ATAC-seq signal in promoters was quantified as the number of fragments mapping to the window 400 bp upstream to 100 bp downstream of the TSS. For motif analysis, the Motifmatchr R package was used to identify motifs from the JASPAR 2016 database (Mathelier et al., 2016) using a p value threshold of 10^{-4}. Accessibility scores for promoters and motif-containing promoters were determined using chromVAR (Schep et al., 2017). Nucleosome positions were determined using NucleoATAC (Schep et al., 2015), and the first nucleosome at least 50 bp upstream of the TSS was identified as the −1 nucleosome and the first nucleosome downstream of that position as the +1 nucleosome.

Analysis of DNA Content and Budding Index

Cells were fixed with 70% ethanol and treated with RNase A and proteinase K prior to staining with Sytox Green at 2 μM in 50 mM sodium citrate (pH 7.4). DNA content was analyzed using a flow cytometer. The budding percentage was calculated as number budded/total cells (minimum of 400 counted per time point).

DATA AND SOFTWARE AVAILABILITY

The accession number for the RNA-seq and ATAC-seq data reported in this paper is NCBI: GSE101290.

Supplementary Material

Refer to Web version on PubMed Central for supplementary material.

Acknowledgments

This work was funded by NIH R35GM119580 (to A.J.M.). We thank the Department of Genetics Bootcamp for technical assistance with ATAC-seq sample processing.

References

Amariei C, Machné R, Stolc V, Soga T, Tomita M, Murray DB. Time resolved DNA occupancy dynamics during the respiratory oscillation uncover a global reset point in the yeast growth program. Microb Cell. 2014; 1:279–288. [PubMed: 28357254]

Beck T, Hall MN. The TOR signalling pathway controls nuclear localization of nutrient-regulated transcription factors. Nature. 1999; 402:689–692. [PubMed: 10604478]

Bosio MC, Fermi B, Spagnoli G, Levati E, Rubbi L, Ferrari R, Pellegrini M, Dieci G. Abf1 and other general regulatory factors control ribosome biogenesis gene expression in budding yeast. Nucleic Acids Res. 2017; 45:4493–4506. [PubMed: 28158860]

Buenrostro JD, Wu B, Litzenburger UM, Ruff D, Gonzales ML, Snyder MP, Chang HY, Greenleaf WJ. Single-cell chromatin accessibility reveals principles of regulatory variation. Nature. 2015; 523:486–490. [PubMed: 26083756]

Burnetti AJ, Aydin M, Buchler NE. Cell cycle Start is coupled to entry into the yeast metabolic cycle across diverse strains and growth rates. Mol Biol Cell. 2016; 27:64–74. [PubMed: 26538026]

Cai L, Sutter BM, Li B, Tu BP. Acetyl-CoA induces cell growth and proliferation by promoting the acetylation of histones at growth genes. Mol Cell. 2011; 42:426–437. [PubMed: 21596309]

Cancer Genome Atlas Research Network. Comprehensive genomic characterization of squamous cell lung cancers. Nature. 2012; 489:519–525. [PubMed: 22960745]

Cancer Genome Atlas Research Network. Comprehensive molecular characterization of urothelial bladder carcinoma. Nature. 2014; 507:315–322. [PubMed: 24476821]

Centers for Disease Control and Prevention. Leading causes of death and numbers of deaths, by sex, race, and Hispanic origin: United States, 1980 and 2014. 2015. http://www.cdc.gov/nchs/hus/contents2015.htm#019

Chambers AL, Ormerod G, Durley SC, Sing TL, Brown GW, Kent NA, Downs JA. The INO80 chromatin remodeling complex prevents polyploidy and maintains normal chromatin structure at centromeres. Genes Dev. 2012; 26:2590–2603. [PubMed: 23207916]

Chen Z, Odstrcil EA, Tu BP, McKnight SL. Restriction of DNA replication to the reductive phase of the metabolic cycle protects genome integrity. Science. 2007; 316:1916–1919. [PubMed: 17600220]

Elfving N, Chereji RV, Bharatula V, Björklund S, Morozov AV, Broach JR. A dynamic interplay of nucleosome and Msn2 binding regulates kinetics of gene activation and repression following stress. Nucleic Acids Res. 2014; 42:5468–5482. [PubMed: 24598258]

Galdieri L, Zhang T, Rogerson D, Vancura A. Reduced Histone Expression or a Defect in Chromatin Assembly Induces Respiration. Mol Cell Biol. 2016; 36:1064–1077. [PubMed: 26787838]

Ganapathi M, Palumbo MJ, Ansari SA, He Q, Tsui K, Nislow C, Morse RH. Extensive role of the general regulatory factors, Abf1 and Rap1, in determining genome-wide chromatin structure in budding yeast. Nucleic Acids Res. 2011; 39:2032–2044. [PubMed: 21081559]

Gasch AP, Spellman PT, Kao CM, Carmel-Harel O, Eisen MB, Storz G, Botstein D, Brown PO. Genomic expression programs in the response of yeast cells to environmental changes. Mol Biol Cell. 2000; 11:4241–4257. [PubMed: 11102521]

Gerhold CB, Gasser SM. INO80 and SWR complexes: relating structure to function in chromatin remodeling. Trends Cell Biol. 2014; 24:619–631. [PubMed: 25088669]

Ghaemmaghami S, Huh WK, Bower K, Howson RW, Belle A, Dephoure N, O'Shea EK, Weissman JS. Global analysis of protein expression in yeast. Nature. 2003; 425:737–741. [PubMed: 14562106]

González A, Shimobayashi M, Eisenberg T, Merle DA, Pendl T, Hall MN, Moustafa T. TORC1 promotes phosphorylation of ribosomal protein S6 via the AGC kinase Ypk3 in Saccharomyces cerevisiae. PLoS ONE. 2015; 10:e0120250. [PubMed: 25767889]

Gut P, Verdin E. The nexus of chromatin regulation and intermediary metabolism. Nature. 2013; 502:489–498. [PubMed: 24153302]

Hartley PD, Madhani HD. Mechanisms that specify promoter nucleosome location and identity. Cell. 2009; 137:445–458. [PubMed: 19410542]

Huang W, Sherman BT, Lempicki RA. Bioinformatics enrichment tools: paths toward the comprehensive functional analysis of large gene lists. Nucleic Acids Res. 2009a; 37:1–13. [PubMed: 19033363]

Huang W, Sherman BT, Lempicki RA. Systematic and integrative analysis of large gene lists using DAVID bioinformatics resources. Nat Protoc. 2009b; 4:44–57. [PubMed: 19131956]

Huber A, Bodenmiller B, Uotila A, Stahl M, Wanka S, Gerrits B, Aebersold R, Loewith R. Characterization of the rapamycin-sensitive phosphoproteome reveals that Sch9 is a central coordinator of protein synthesis. Genes Dev. 2009; 23:1929–1943. [PubMed: 19684113]

Huber A, French SL, Tekotte H, Yerlikaya S, Stahl M, Perepelkina MP, Tyers M, Rougemont J, Beyer AL, Loewith R. Sch9 regulates ribosome biogenesis via Stb3, Dot6 and Tod6 and the histone deacetylase complex RPD3L. EMBO J. 2011; 30:3052–3064. [PubMed: 21730963]

Kasinathan S, Orsi GA, Zentner GE, Ahmad K, Henikoff S. High-resolution mapping of transcription factor binding sites on native chromatin. Nat Methods. 2014; 11:203–209. [PubMed: 24336359]

Klevecz RR, Bolen J, Forrest G, Murray DB. A genomewide oscillation in transcription gates DNA replication and cell cycle. Proc Natl Acad Sci USA. 2004; 101:1200–1205. [PubMed: 14734811]

Koerber RT, Rhee HS, Jiang C, Pugh BF. Interaction of transcriptional regulators with specific nucleosomes across the Saccharomyces genome. Mol Cell. 2009; 35:889–902. [PubMed: 19782036]

Kuang Z, Cai L, Zhang X, Ji H, Tu BP, Boeke JD. High-temporal-resolution view of transcription and chromatin states across distinct metabolic states in budding yeast. Nat Struct Mol Biol. 2014; 21:854–863. [PubMed: 25173176]

Kuang Z, Pinglay S, Ji H, Boeke JD. Msn2/4 regulate expression of glycolytic enzymes and control transition from quiescence to growth. eLife. 2017; 6:e29938. [PubMed: 28949295]

Laplante M, Sabatini DM. mTOR signaling at a glance. J Cell Sci. 2009; 122:3589–3594. [PubMed: 19812304]

Laxman S, Sutter BM, Tu BP. Behavior of a metabolic cycling population at the single cell level as visualized by fluorescent gene expression reporters. PLoS ONE. 2010; 5:e12595. [PubMed: 20830298]

Lempiäinen H, Uotila A, Urban J, Dohnal I, Ammerer G, Loewith R, Shore D. Sfp1 interaction with TORC1 and Mrs6 reveals feedback regulation on TOR signaling. Mol Cell. 2009; 33:704–716. [PubMed: 19328065]

López-Maury L, Marguerat S, Bähler J. Tuning gene expression to changing environments: from rapid responses to evolutionary adaptation. Nat Rev Genet. 2008; 9:583–593. [PubMed: 18591982]

Love MI, Huber W, Anders S. Moderated estimation of fold change and dispersion for RNA-seq data with DESeq2. Genome Biol. 2014; 15:550. [PubMed: 25516281]

Machné R, Murray DB. The yin and yang of yeast transcription: elements of a global feedback system between metabolism and chromatin. PLoS ONE. 2012; 7:e37906. [PubMed: 22685547]

Marion RM, Regev A, Segal E, Barash Y, Koller D, Friedman N, O'Shea EK. Sfp1 is a stress- and nutrient-sensitive regulator of ribosomal protein gene expression. Proc Natl Acad Sci USA. 2004; 101:14315–14322. [PubMed: 15353587]

Martínez-Pastor MT, Marchler G, Schüller C, Marchler-Bauer A, Ruis H, Estruch F. The Saccharomyces cerevisiae zinc finger proteins Msn2p and Msn4p are required for transcriptional induction through the stress response element (STRE). EMBO J. 1996; 15:2227–2235. [PubMed: 8641288]

Mathelier A, Fornes O, Arenillas DJ, Chen CY, Denay G, Lee J, Shi W, Shyr C, Tan G, Worsley-Hunt R, et al. JASPAR 2016: a major expansion and update of the open-access database of transcription factor binding profiles. Nucleic Acids Res. 2016; 44(D1):D110–D115. [PubMed: 26531826]

Matsuo T, Yamaguchi S, Mitsui S, Emi A, Shimoda F, Okamura H. Control mechanism of the circadian clock for timing of cell division in vivo. Science. 2003; 302:255–259. [PubMed: 12934012]

McAdams HH, Shapiro L. A bacterial cell-cycle regulatory network operating in time and space. Science. 2003; 301:1874–1877. [PubMed: 14512618]

Mizuguchi G, Shen X, Landry J, Wu WH, Sen S, Wu C. ATP-driven exchange of histone H2AZ variant catalyzed by SWR1 chromatin remodeling complex. Science. 2004; 303:343–348. [PubMed: 14645854]

Morrison AJ, Shen X. Chromatin remodelling beyond transcription: the INO80 and SWR1 complexes. Nat Rev Mol Cell Biol. 2009; 10:373–384. [PubMed: 19424290]

Morrison AJ, Kim JA, Person MD, Highland J, Xiao J, Wehr TS, Hensley S, Bao Y, Shen J, Collins SR, et al. Mec1/Tel1 phosphorylation of the INO80 chromatin remodeling complex influences DNA damage checkpoint responses. Cell. 2007; 130:499–511. [PubMed: 17693258]

Murray DB, Beckmann M, Kitano H. Regulation of yeast oscillatory dynamics. Proc Natl Acad Sci USA. 2007; 104:2241–2246. [PubMed: 17284613]

Nagoshi E, Saini C, Bauer C, Laroche T, Naef F, Schibler U. Circadian gene expression in individual fibroblasts: cell-autonomous and self-sustained oscillators pass time to daughter cells. Cell. 2004; 119:693–705. [PubMed: 15550250]

Nocetti N, Whitehouse I. Nucleosome repositioning underlies dynamic gene expression. Genes Dev. 2016; 30:660–672. [PubMed: 26966245]

Panda S. Circadian physiology of metabolism. Science. 2016; 354:1008–1015. [PubMed: 27885007]

Papagiannakis A, Niebel B, Wit EC, Heinemann M. Autonomous Metabolic Oscillations Robustly Gate the Early and Late Cell Cycle. Mol Cell. 2017; 65:285–295. [PubMed: 27989441]

Rao AR, Pellegrini M. Regulation of the yeast metabolic cycle by transcription factors with periodic activities. BMC Syst Biol. 2011; 5:160. [PubMed: 21992532]

Ringnér M. What is principal component analysis? Nat Biotechnol. 2008; 26:303–304. [PubMed: 18327243]

Robertson JB, Stowers CC, Boczko E, Johnson CH. Real-time luminescence monitoring of cell-cycle and respiratory oscillations in yeast. Proc Natl Acad Sci USA. 2008; 105:17988–17993. [PubMed: 19004762]

Sardiu ME, Gilmore JM, Groppe B, Florens L, Washburn MP. Identification of Topological Network Modules in Perturbed Protein Interaction Networks. Sci Rep. 2017; 7:43845. [PubMed: 28272416]

Schep AN, Buenrostro JD, Denny SK, Schwartz K, Sherlock G, Greenleaf WJ. Structured nucleosome fingerprints enable high-resolution mapping of chromatin architecture within regulatory regions. Genome Res. 2015; 25:1757–1770. [PubMed: 26314830]

Schep AN, Wu B, Buenrostro JD, Greenleaf WJ. chromVAR: inferring transcription-factor-associated accessibility from single-cell epigenomic data. Nat Methods. 2017; 14:975–978. [PubMed: 28825706]

Schmitt AP, McEntee K. Msn2p, a zinc finger DNA-binding protein, is the transcriptional activator of the multistress response in Saccharomyces cerevisiae. Proc Natl Acad Sci USA. 1996; 93:5777–5782. [PubMed: 8650168]

Shen X, Mizuguchi G, Hamiche A, Wu C. A chromatin remodelling complex involved in transcription and DNA processing. Nature. 2000; 406:541–544. [PubMed: 10952318]

Shen X, Ranallo R, Choi E, Wu C. Involvement of actin-related proteins in ATP-dependent chromatin remodeling. Mol Cell. 2003; 12:147–155. [PubMed: 12887900]

Silverman SJ, Petti AA, Slavov N, Parsons L, Briehof R, Thiberge SY, Zenklusen D, Gandhi SJ, Larson DR, Singer RH, Botstein D. Metabolic cycling in single yeast cells from unsynchronized steady-state populations limited on glucose or phosphate. Proc Natl Acad Sci USA. 2010; 107:6946–6951. [PubMed: 20335538]

Tosi A, Haas C, Herzog F, Gilmozzi A, Berninghausen O, Ungewickell C, Gerhold CB, Lakomek K, Aebersold R, Beckmann R, Hopfner KP. Structure and subunit topology of the INO80 chromatin remodeler and its nucleosome complex. Cell. 2013; 154:1207–1219. [PubMed: 24034245]

Tu BP, Kudlicki A, Rowicka M, McKnight SL. Logic of the yeast metabolic cycle: temporal compartmentalization of cellular processes. Science. 2005; 310:1152–1158. [PubMed: 16254148]

Urban J, Soulard A, Huber A, Lippman S, Mukhopadhyay D, Deloche O, Wanke V, Anrather D, Ammerer G, Riezman H, et al. Sch9 is a major target of TORC1 in Saccharomyces cerevisiae. Mol Cell. 2007; 26:663–674. [PubMed: 17560372]

Wagner A. Energy constraints on the evolution of gene expression. Mol Biol Evol. 2005; 22:1365–1374. [PubMed: 15758206]

Wang Q, Donze D. Transcription factor Reb1 is required for proper transcriptional start site usage at the divergently transcribed TFC6-ESC2 locus in Saccharomyces cerevisiae. Gene. 2016; 594:108–116. [PubMed: 27601258]

Wang GZ, Hickey SL, Shi L, Huang HC, Nakashe P, Koike N, Tu BP, Takahashi JS, Konopka G. Cycling Transcriptional Networks Optimize Energy Utilization on a Genome Scale. Cell Rep. 2015; 13:1868–1880. [PubMed: 26655902]

Wanke V, Cameroni E, Uotila A, Piccolis M, Urban J, Loewith R, De Virgilio C. Caffeine extends yeast lifespan by targeting TORC1. Mol Microbiol. 2008; 69:277–285. [PubMed: 18513215]

Warner JR. The economics of ribosome biosynthesis in yeast. Trends Biochem Sci. 1999; 24:437–440. [PubMed: 10542411]

Watanabe S, Tan D, Lakshminarasimhan M, Washburn MP, Hong EJ, Walz T, Peterson CL. Structural analyses of the chromatin remodelling enzymes INO80-C and SWR-C. Nat Commun. 2015; 6:7108. [PubMed: 25964121]

Witkiewicz AK, McMillan EA, Balaji U, Baek G, Lin WC, Mansour J, Mollaee M, Wagner KU, Koduru P, Yopp A, et al. Whole-exome sequencing of pancreatic cancer defines genetic diversity and therapeutic targets. Nat Commun. 2015; 6:6744. [PubMed: 25855536]

Yao W, Beckwith SL, Zheng T, Young T, Dinh VT, Ranjan A, Morrison AJ. Assembly of the Arp5 (Actin-related Protein) Subunit Involved in Distinct INO80 Chromatin Remodeling Activities. J Biol Chem. 2015; 290:25700–25709. [PubMed: 26306040]

Yao W, King DA, Beckwith SL, Gowans GJ, Yen K, Zhou C, Morrison AJ. The INO80 Complex Requires the Arp5-Ies6 Subcomplex for Chromatin Remodeling and Metabolic Regulation. Mol Cell Biol. 2016; 36:979–991. [PubMed: 26755556]

Yen K, Vinayachandran V, Batta K, Koerber RT, Pugh BF. Genome-wide nucleosome specificity and directionality of chromatin remodelers. Cell. 2012; 149:1461–1473. [PubMed: 22726434]

Yerlikaya S, Meusburger M, Kumari R, Huber A, Anrather D, Costanzo M, Boone C, Ammerer G, Baranov PV, Loewith R. TORC1 and TORC2 work together to regulate ribosomal protein S6 phosphorylation in Saccharomyces cerevisiae. Mol Biol Cell. 2016; 27:397–409. [PubMed: 26582391]

Zaslaver A, Mayo AE, Rosenberg R, Bashkin P, Sberro H, Tsalyuk M, Surette MG, Alon U. Just-in-time transcription program in metabolic pathways. Nat Genet. 2004; 36:486–491. [PubMed: 15107854]

Zhang R, Lahens NF, Ballance HI, Hughes ME, Hogenesch JB. A circadian gene expression atlas in mammals: implications for biology and medicine. Proc Natl Acad Sci USA. 2014; 111:16219–16224. [PubMed: 25349387]

Highlights

- The INO80 complex controls cellular respiration in *S. cerevisiae*
- Cell division is disconnected from energy metabolism in INO80 mutants
- INO80 mutants exhibit globally altered gene expression and chromatin accessibility
- INO80 regulates downstream TORC1-responsive gene expression

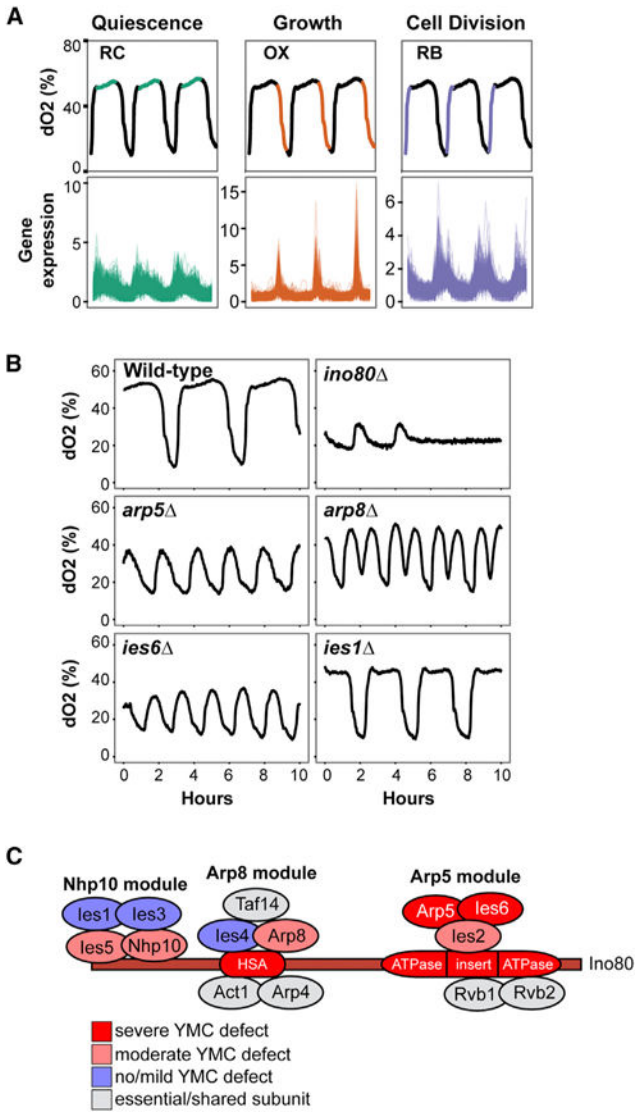

Figure 1. The INO80 Complex Is Essential for Respiration Oscillations

(A) Organization of the yeast metabolic cycle (YMC). Top: respiration cycles are shown with the corresponding percentage of dissolved oxygen (dO_2) in culture. Bottom: relative fold change gene expression of previously classified periodic genes (Tu et al., 2005). RC, reductive charging (1,508 periodic genes); OX, oxidative (1,016 periodic genes); RB, reductive building (975 periodic genes).

(B) dO_2 traces in the wild-type and indicated mutant strains lacking subunits of the INO80 complex.

(C) Illustration of the INO80 complex with structural modules noted fromTosi et al. (2013). Colors denote the severity of YMC defects observed upon deletion of the indicated subunit. See also Figure S1 and Table S1.

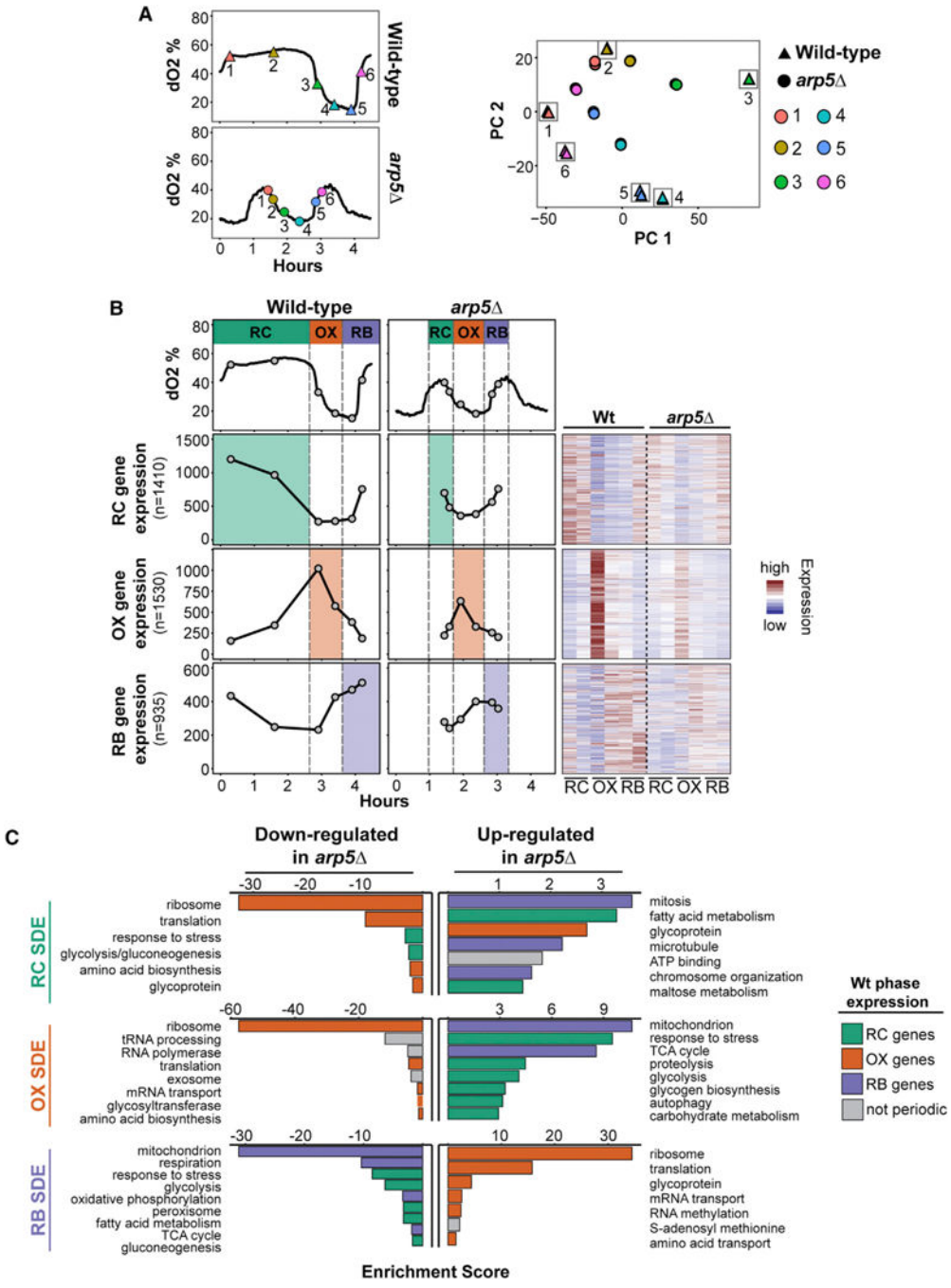

Figure 2. Disruption of the INO80 Complex Alters Global Transcription across the YMC

(A) Left: YMC dO_2 traces in the wild-type and *arp5Δ* mutant. Samples were taken at the indicated time points (coded by color) for RNA-seq and PCA. Right: principal components (PCs) 1 and 2 are shown. Technical replicates are displayed for each time point and separated by strain.

(B) Left: mean expression of periodic genes in wild-type (WT) and *arp5Δ* strains within each YMC phase. n = number of periodic genes in each phase previously classified (Kuang

et al., 2014). Expression of each gene is shown as FPKM. Right: expression of each individual gene is shown as heatmaps (scaled by row).

(C) DAVID functional enrichment analysis of significantly differentially expressed (SDE) genes at comparable time points between the wild-type and *arp5Δ* mutant (refer to Experimental Procedures for more detail). Bar colors denote the wild-type phase with which periodic genes are associated.

Enrichment scores are −log10(p value). See also Table S2.

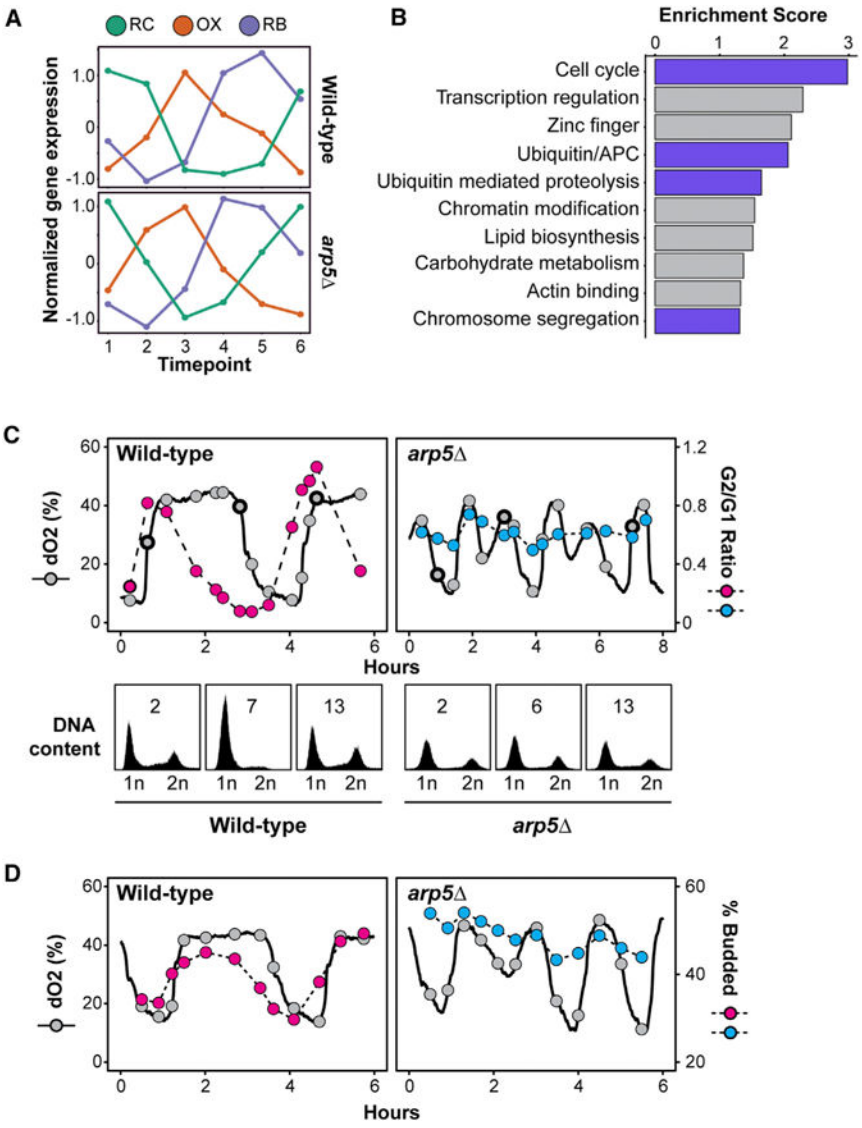

Figure 3. Cell Division Is Disconnected from the YMC in the arp5Δ Mutant

(A) *k*-means clustering of previously classified periodic genes (Kuang et al., 2014) following z-score normalization of RNA-seq data for each gene, time point, and strain.

(B) DAVID functional enrichment of genes in the *arp5Δ* mutant that do not cluster in the corresponding YMC phase. Annotations related to cell cycle are highlighted. APC, anaphase-promoting complex. Enrichment scores are −log10(p value).

(C) Samples were taken at indicated time points across wild-type and *arp5Δ* YMCs. Top: dO_2 traces and ratio of G2 to G1 cells for each strain. Bottom: representative DNA content histograms from samples indicated with a thicker outline at the top.

(D) Number of budding cells, indicative of M phase entry, in samples across wild-type and *arp5Δ* YMCs.

See also Table S3.

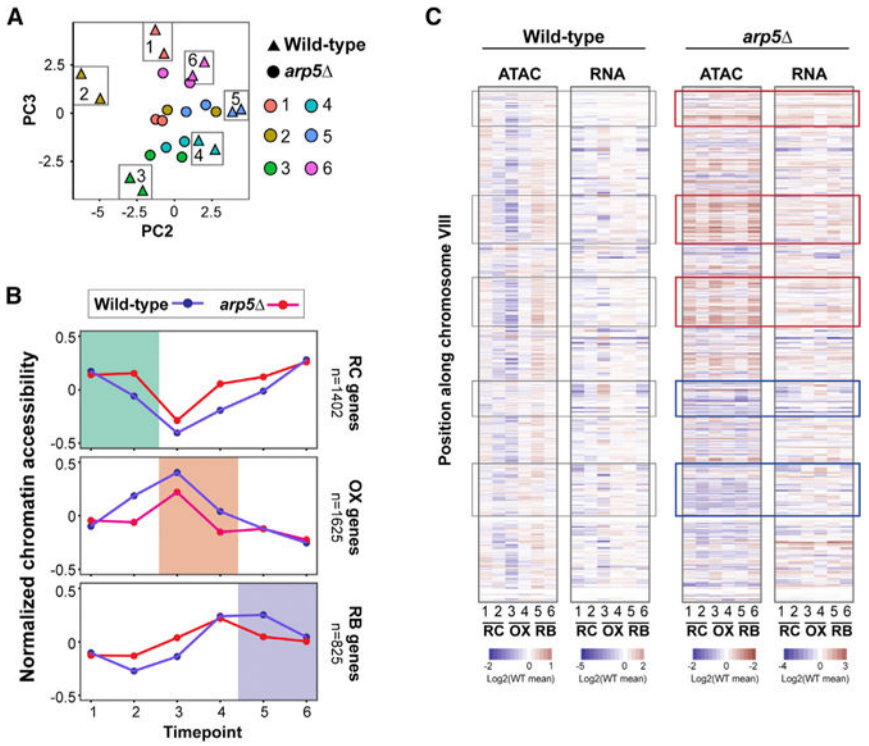

Figure 4. Loss of INO80 Function Alters Global Chromatin Accessibility in the YMC

(A) PCA plot of ATAC-seq data from samples taken at time points shown in Figure 2A. Replicates are displayed for each time point and strain (colored as in Figure 2A).

(B) Comparison of mean ATAC-seq scores for periodic genes from each phase of wild-type and *arp5Δ* YMC following *Z* score normalization for each gene and time point. The RC, OX, and RB phases are highlighted.

(C) Chromosomal plot of $\log_2$ mean wild-type and *arp5Δ* ATAC-seq and RNA-seq (FPKM) in 500 bp bins for the YMC time points described in Figure 2A. Scores in both wild-type and *arp5Δ* cells were normalized to mean wild-type. Red and blue boxes highlight static regions of increased and decreased accessibility, respectively, in *arp5Δ* cells. Gray boxes indicate the corresponding chromosomal regions in wild-type cells.

See also Figures S2 and S3.

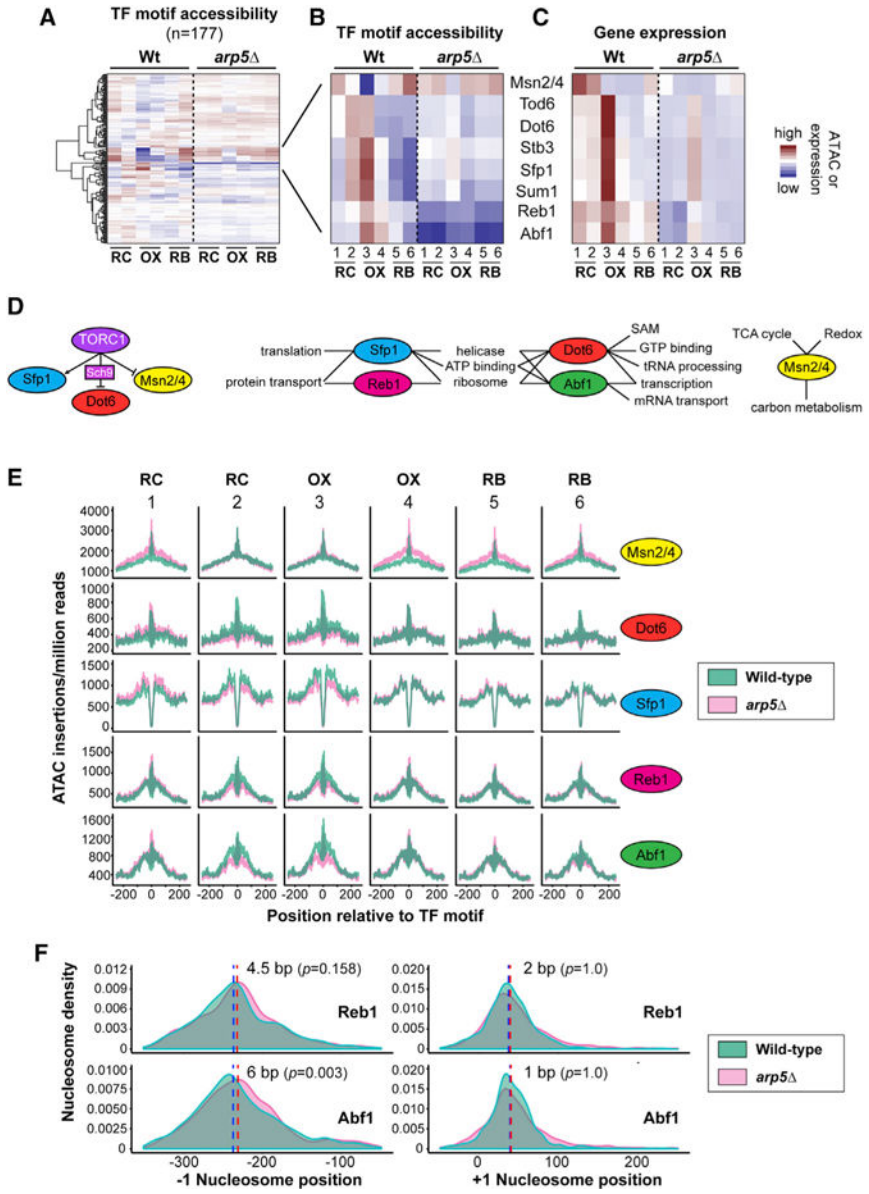

Figure 5. Metabolic Gene Promoters Are Dependent on INO80-Regulated Chromatin Accessibility

(A) Promoter ATAC accessibility scores organized by all annotated transcription factor (TF) motifs are shown for both wild-type and *arp5Δ* YMCs.

(B) Magnification of indicated region in (A). The time points and YMC phase from Figure 2A are shown.

(C) Mean RNA-seq FPKM for genes that contain the indicated transcription factor motifs in their promoters.

(D) Left: illustration of the TORC1 pathway for the indicated transcription factors. Right: DAVID significant functional enrichment of genes with the indicated transcription factor motifs. SAM, S-adenosyl-methionine; TCA, tricarboxylic acid.

(E) ATAC accessibility is shown as the number of Tn5 insertions per million reads around the indicated transcription factor motif for wild-type (green) and *arp5Δ* (pink) samples.

(F) +1 and −1 nucleosome densities, relative to transcription start sites, containing Abf1 or Reb1 motifs. Wild-type (green) and *arp5Δ* (pink) samples across all time points of the YMC are shown. Red/blue dotted lines denote the median nucleosome position for the wild-type and *arp5Δ*, respectively. p = 0.002 for Abf1 and 0.158 for Reb1.
See also Figure S4.

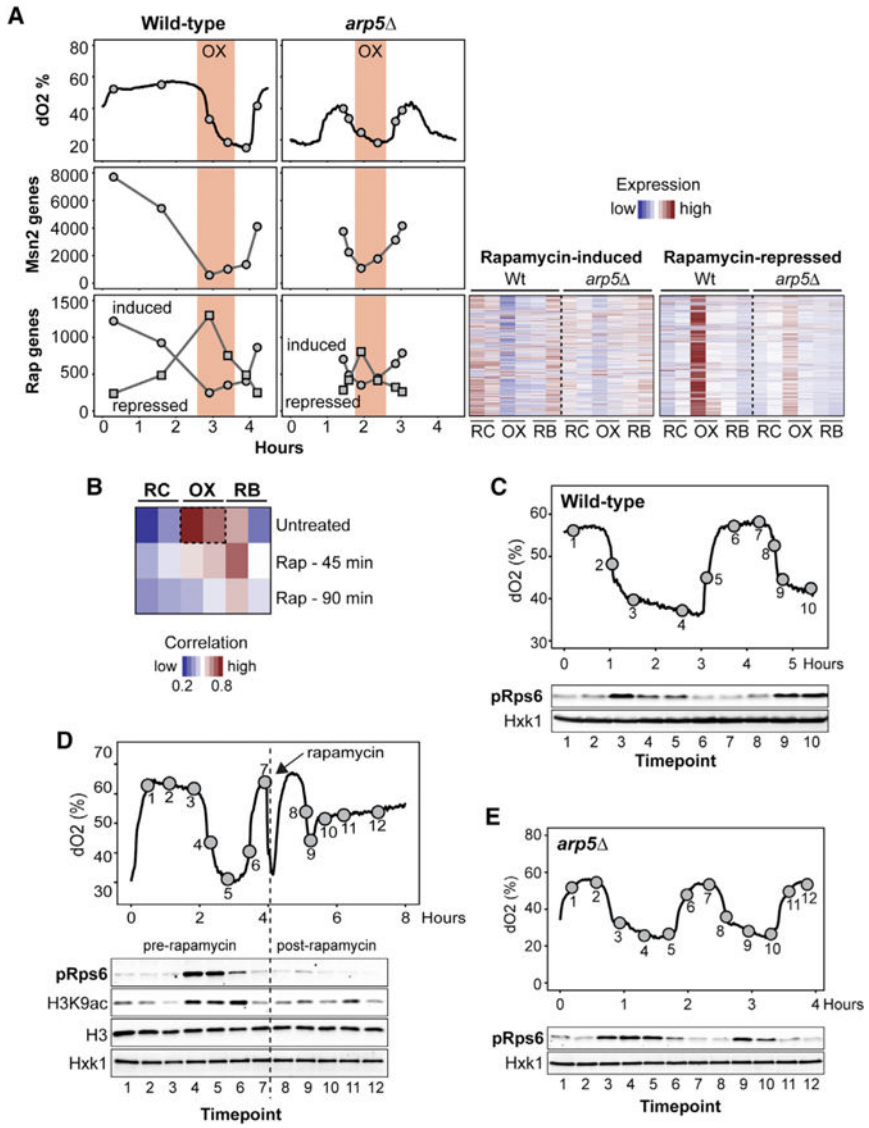

Figure 6. The INO80 Complex Is a Key Regulator of TORC1-Responsive Gene Expression

(A) Top: same as Figure 2A. YMC dO_2 traces in the wild-type and *arp5Δ* mutant. RNA-seq samples were taken at the indicated time points. Mean expression is shown as FPKM of Msn2-induced genes (center, Msn2 genes) and rapamycin-sensitive genes (bottom, Rap genes) across the YMC. Right: gene expression heatmaps of rapamycin-sensitive genes scaled by row.

(B) Pearson's correlation between the RNA transcript levels across the wild-type YMC and those in an asynchronous culture before and after rapamycin treatment (30 nM) for the indicated time in minutes.

(C) Western blot analysis of the indicated wild-type time points with an antibody that recognizes the phosphorylated TORC1 substrate, mammalian homolog ribosomal protein S6 (Rps6). Hexokinase 1 (Hxk1) is shown as a loading control.

(D) Samples were taken across a wild-type YMC at the indicated time points before and after treatment with rapamycin (50 nM), indicated by the dashed line. Also shown is a

western blot analysis using antibodies that recognize pRps6, Hxk1, acetylated histone H3 lysine 9, (H3K9ac), and histone H3 (H3).

(E) Western blot analysis of the *arp5Δ* mutant YMC as in (C).

See also Figure S5 and Table S4.